PRAMANA — journal of physics

Vol. 77, No. 5
November 2011
pp. 817–826

Learning and structure of neuronal networks

KIRAN M KOLWANKAR[1,2,*], QUANSHENG REN[2,3], AREEJIT SAMAL[2,4] and JÜRGEN JOST[2,5]

[1]Department of Physics, Ramniranjan Jhunjhunwala College, Ghatkopar (W), Mumbai 400 086, India
[2]Max Planck Institute for Mathematics in the Sciences, Inselstr. 22, 04103 Leipzig, Germany
[3]School of Electronics Engineering and Computer Science, Peking University, Beijing 100871, China
[4]Laboratoire de Physique Théorique et Modèles Statistiques, CNRS and Univ Paris-Sud, UMR 8626, F-91405 Orsay, France
[5]Santa Fe Institute, 1399 Hyde Park Road, Santa Fe, NM 87501, USA
*Corresponding author. E-mail: Kiran.Kolwankar@gmail.com

Abstract. We study the effect of learning dynamics on network topology. Firstly, a network of discrete dynamical systems is considered for this purpose and the coupling strengths are made to evolve according to a temporal learning rule that is based on the paradigm of spike-time-dependent plasticity (STDP). This incorporates necessary competition between different edges. The final network we obtain is robust and has a broad degree distribution. Then we study the dynamics of the structure of a formal neural network. For properly chosen input signals, there exists a steady state with a residual network. We compare the motif profile of such a network with that of the real neural network of *C. elegans* and identify robust qualitative similarities. In particular, our extensive numerical simulations show that this STDP-driven resulting network is robust under variations of model parameters.

Keywords. Neuronal networks; scale-free network; synapses; learning; logistic map.

PACS Nos 87.18.Sn; 87.19.lv; 05.45.Xt; 89.75.Hc

1. Introduction

Complex networks are ubiquitous in nature. Several phenomena in nature, such as brain structures, protein–protein interaction networks, social interactions, the Internet, and so on can be described by complex networks [1–5]. Recent developments in the understanding of complex networks has led to deeper insights about their origin and other properties [1–5]. One common realization that emerges from these studies is that different types of networks have different origins and there is no unifying principle. As a result, one needs to study various possible ways to construct robust networks, and also figure out dominant factors that give rise to specific networks.

We focus here on the structure and dynamics of neuronal networks. Progress in the understanding of complex networks has also led to a parallel activity in the area of neural

DOI: 10.1007/s12043-011-0192-2; ***e*Publication: 31 October 2011**

networks which showed that the network in the brain possesses small-world and scale-free properties [6,7]. Further, a network motif [8] analysis of the *C. elegans* neural network showed that it belongs to one of the four superfamilies [9] of networks.

These developments lead to a natural question about the factors that determine the observed network structure in the brain. The purpose of this paper is to review some of our previous work [10–11] which addresses this issue. Our earlier work [10–11] showed that the mechanism of learning, that is, the modification of the coupling strengths dependent upon the dynamics of the neurons play a crucial role in determining the observed neural network structure.

This review is organized as follows. Section 2 recalls the relevant biological findings. We then describe different neural network models considered in §3. Section 4 discusses our earlier results. The paper then ends with a section on concluding remarks.

2. Biological background

In the brain, neuronal networks are formed by neurons connected to each other via directed synapses that transmit electrical signals between neurons. The potential of a neuron changes on a fast time-scale depending on the inputs from other neurons. The strength of a synapse determines its efficiency to transmit a signal. The dynamics of synaptic strengths which is interpreted as learning is much slower than the dynamics of the neurons (see, e.g. ref. [12]).

It is well known that just after birth, the brain has a very dense population of synaptic connections and, as time progresses, most of the synaptic connections are pruned [13]. The pruning is not restricted to larger brains but also occurs in the brain of a small worm like *C. elegans* [14]. This leads to the question about the role played by learning dynamics in determining the final neural network structure.

The neural network of the worm *C. elegans* is completely known [15]. Further, there exists some variation in the neural network structure from animal to animal [16]. The neural network of *C. elegans* has been studied extensively in the literature [17,18]. It was found that perturbed sensory activity and mutations altering the calcium channels or membrane potential affect the axon outgrowth [19] implying that the neural network is not genetically hard wired. In ref. [6], using functional magnetic resonance imaging data, it was shown that the functional networks in the brain have small-world and scale-free properties.

Spike-timing-dependent plasticity (STDP) is an experimentally observed biological process that adjusts the strength of synaptic connections between neurons in the brain [20]. The process adjusts the connection strengths based on the relative timing of a particular neuron's output and input action potentials (or spikes). In this study, the weight of the synaptic connection is modified by a STDP motivated rule.

3. Description of models

3.1 *Discrete nonlinear map*

We study the following coupled dynamical system

$$X_{n+1} = Gf(X_n), \tag{1}$$

where X_n is an N-dimensional column vector representing the state of nodes in the network, G is an $N \times N$ coupling matrix describing the connectivity of the network and f is a map from $\Omega = [0, 1]^N$ onto itself modelling the dynamics of the node. We consider chaotic dynamics via the logistic map defined as

$$f(x) = \mu x(1 - x) \tag{2}$$

with $\mu = 4$. $G_{ij}(i \neq j)$ is the coupling strength of the edge from j to i, and we impose the balancing condition $G_{ii} = 1 - \sum_{i \neq j} G_{ij}$. $G_{ij} = 0$ signifies that there is no link from j to i. Note that we choose G_{ij} for $i \neq j$ to be nonnegative, i.e., we do not consider inhibitory synapses.

For the above-mentioned discrete dynamical system, the learning rule also has to be discrete. We choose the following learning rule:

$$G_{ij}(n + 1) = G_{ij}(n) + \epsilon(X_j(n - 1)X_i(n) - X_j(n)X_i(n - 1)), \tag{3}$$

where ϵ is a small parameter deciding the time-scale of the learning dynamics. Thus, the strength of the connection from j to i grows when the state of j at time $n-1$ and the state of i at time n are correlated, and it decreases when the correlation switches the temporal order, i.e., when i is active before j. Hence, this rule represents a discrete time implementation of STDP. When two nodes are synchronized in the network, the coupling strength between them does not change. From a different perspective, in connection with information flows in networks, a general class of such learning rules has been considered in ref. [21].

3.2 *Realistic neuronal dynamics*

We have studied two realistic neuronal models using the NEST simulation tool [22]: the leaky integrate-and-fire (LIF) model and the Hodgkin–Huxley (HH) model. The parameter values for our simulations of the LIF model were taken from ref. [23] and that for the HH model from ref. [24]. We do not consider inhibitory synapses which are extremely rare between interneurons in the *C. elegans* network [16]. In both models, the synaptic conductance $g_i(t)$ is given by $g_i(t) = g_m \sum_{j=1}^{N} w_{ij}(t) \sum_k f(t - t_j^k)$, where N is the number of neurons, g_m is the maximum value of the synaptic conductance, w_{ij} is the weight of the synaptic connection from neuron i to neuron j, t_j^k is the timing of the kth spike of neuron j.

The amount of synaptic weight modification is determined by the temporal difference Δt between the occurrence of the postsynaptic action potential and the arrival of the presynaptic action potential via a STDP learning rule. $\Delta t = t_j - (t_i + \tau_d)$, where t_j is the spike time of the postsynaptic neuron j, τ_d is the time delay of the spike transmission from neuron i to neuron j and t_i is the spike time of the presynaptic neuron i. The weight modification Δw_{ij} is described by the following equations:

$$\Delta w_{ij}(\Delta t) = \begin{cases} \lambda \exp(-|\Delta t|/\tau_+) & \text{if } \Delta t \geq \tau_d \\ -\lambda\alpha \exp(-|\Delta t|/\tau_-) & \text{if } \Delta t < \tau_d, \end{cases} \tag{4}$$

where the learning rate $\lambda = 0.0001$ and w_{ij} are constrained in the range $[0, 1]$. α introduces a possible asymmetry between the scale of potentiation and depression and the time constants τ_+ and τ_- control the width of the time window.

4. Results and discussion

4.1 *Logistic map model*

To study the effect of learning on the network topology, we begin with a globally coupled network of discrete dynamical systems described by eqs (1) and (2). The dynamics of the coupling strengths is governed by eq. (3). We assign small nonzero initial values to the coupling strength and allow the system to evolve for about 10^7–2×10^8 time steps depending on the number of nodes in the network. The number of nodes in the network were taken as powers of 2, from 16 to 1024. If the coupling strength of any edge becomes negative, then we clamp it to zero thereafter. This is pruning of the edge. We find that the evolution leads to a steady state with a robust scale-free network.

The initial values of the edge strengths were taken to be distributed randomly (and uniformly) in an interval $[0, g_{\text{in}}^{\max}]$, where $g_{\text{in}}^{\max} = 0.25/(N-1)$. The value of ϵ is much less than $g_{\text{in}}^{\max}$. In figure 1, the number of edges in the network is plotted against the number of iterations. We see that the number of edges decreases very fast in the beginning and then reaches a constant value. We observe that this value is of the order of the number of nodes in the network. The strengths of the remaining edges are then unlikely to become zero, keeping the structure of the final residual network intact. Addition of small random noise to the learning dynamics did not affect the conclusions. Thus, it follows that as the system evolves the coupling strength of many edges drops to zero but at the same time some edges become stronger and their strength attains a steady value. This was found to occur for several values of the system size as well as sufficiently small values of ϵ.

We have studied some properties of the residual network and the robustness of the observed properties to changes in parameter values. We have studied the frequency of

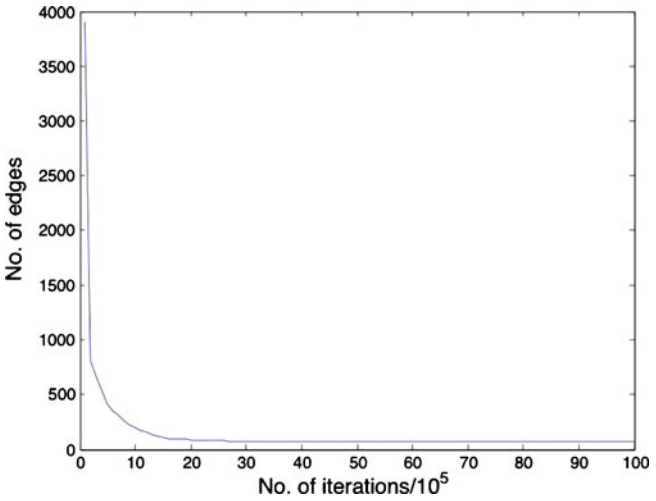

Figure 1. Plot of the number of edges in the network vs. the number of iterations. Here, we have shown the case where number of nodes is 64, $\epsilon = 0.001$ and the number of iterations is 10^7.

different three-node subgraphs in the residual network, which yields information about the local network structure. Out of the 13 possible three-node subgraphs or triads, only four triads are present in the final network irrespective of the value of ϵ and network size. If A, B and C are three different nodes in a triad then the four observed triads are: (1) links going out from (say) B to both A and C, (2) opposite of (1), i.e., links coming into B from both A and C, (3) a link from A to B and from B to C and (4) a cyclic triangle. The other triads are absent in the residual network. In particular, triads with double links, i.e., a link from A to B and also from B to A, are absent. This is expected from the considered learning rule since $G_{ij} + G_{ji}$ is a constant and so the strength of one link grows at the expense of the other. Noncyclic triads are also absent in the residual network.

The most interesting outcome of this study is the final structure of the graph. We find that though some nodes and small clusters get separated there is still a single large connected component. In figure 2 we show the residual graph of 1024 nodes. Its scale-free nature is evident from the broad degree distribution depicted in figure 3. Independently, Shin and Kim [25] have also found a similar result using the FitzHug–Nagumo model.

4.2 *Realistic models*

In this case, we start our simulations of the STDP-driven pruning process with an all-to-all connected network where neurons are stimulated by different periodic patterns repeatedly with period T_{pattern}. We generate all the patterns from Poisson spike trains with the same average firing rate $f_{\text{Poisson}} = 50$ Hz. This average firing rate corresponds to a 20 ms spike interval and is consistent with the width of the STDP time window. In all cases, the peak

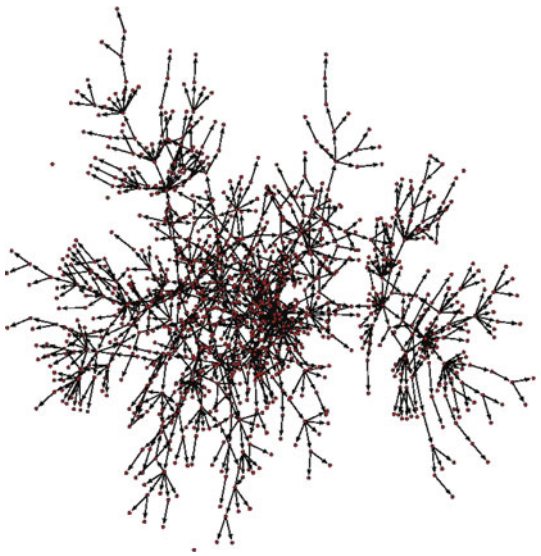

Figure 2. The structure of the final network with 1024 nodes after 2×10^8 iterations. Here, $\epsilon = 0.00005$.

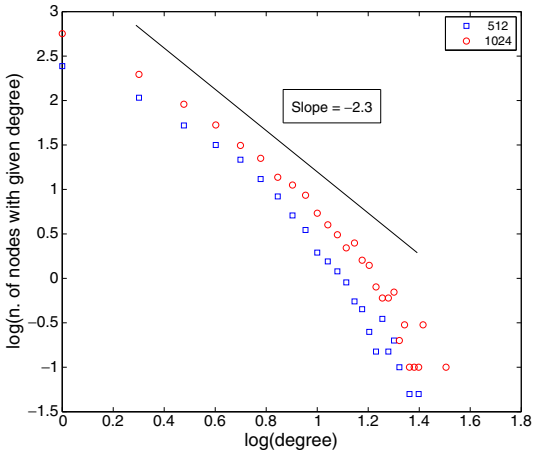

Figure 3. The degree distribution for networks with 512 nodes (blue squares) averaged over 20 realizations and 1024 nodes (red circles) averaged over 10 realizations.

synaptic conductances and the neuron potentials are initialized with a random uniform distribution. Most of the peak synaptic conductances are pushed toward zero or g_{m} after development. The threshold for synaptic pruning is set to $g = 0.005$ nS. We analyse the occurrence of triads in the resulting steady-state network of the investigated LIF and HH neuronal models.

We follow the approach outlined above to study four cases with different configurations. We refer to the first case as 'basic configuration', and the other cases are variations of the first case. In the 'basic configuration', we simulate a network of $N = 100$ LIF neurons which is similar in size to the *C. elegans* subnetwork of somatic interneurons. An asymmetric time window $\tau_+ = 16.8$ ms and $\tau_- = 33.7$ ms was used in the STDP rule which provides a reasonable approximation of the observed synaptic modification in actual experiments [26]. We take $\alpha = 0.525$ along with the asymmetric time window resulting in the ratio $A_-\tau_-/A_+\tau_+ = 1.05$ similar to that in ref. [23]. We set the other parameters as follows: the synaptic delay $\tau_{\mathrm{d}} = 10$ ms, the maximum peak synaptic conductance $g_{\mathrm{m}} = 0.3$ nS, and the period of input patterns $T_{\mathrm{pattern}} = 2$ s. We also study three variations of the 'basic configuration': 'Symmetric configuration', where the asymmetric time window is replaced with a symmetric one ($\tau_+ = \tau_- = 20.0$ ms), and $\alpha = 1.05$ to preserve the ratio $A_-\tau_-/A_+\tau_+ = 1.05$; 'HH model configuration', where LIF model is replaced by the HH model; 'Large network configuration', where the network size is enlarged to 200 neurons and $g_{\mathrm{m}} = 0.2$ nS. For all four cases, we repeat our simulations ten times with different input patterns and initial values.

We have used the Mfinder software [8] developed by U Alon's group to determine the occurrence of three-node subgraphs in our STDP-driven networks. The abundance of each subgraph i is quantified by the Z-score

$$z_i = \frac{N_i^{\mathrm{real}} - \langle N_i^{\mathrm{rand}} \rangle}{\mathrm{std}(N_i^{\mathrm{rand}})},$$

where N_i^{real} is the abundance of subgraph i in the real network, $\langle N_i^{\text{rand}} \rangle$ and std(N_i^{rand}) are the mean and standard deviation of abundance of subgraph i in an ensemble of 1000 random networks generated by preserving the same number of incoming, outgoing and mutual edges at each node compared to the real network. If $z_i > 0$ ($z_i < 0$) then the subgraph i is over-represented (under-represented) and is designated as a motif (antimotif) [8]. The significance profile (SP) of different subgraphs in a network is the vector of Z-scores normalized to length 1:

$$\text{SP}_i = z_i / \sqrt{\sum_{i=1}^{13} z_i^2}.$$

SP shows the relative significance of subgraphs and is important for comparison of networks of different sizes and degree sequences [9].

The SPs of triads for the four configurations mentioned earlier along with that for the *C. elegans* neuronal network is shown in figure 4. It is seen that all four STDP-driven evolved networks have very similar SPs with triads 7, 9 and 10 as motifs, and triads 1, 2, 4 and 5 as antimotifs, as in the SP of the *C. elegans* network which belongs to the second superfamily reported in ref. [9]. The SP curves for the four STDP-driven evolved networks are even more similar to the *C. elegans* subnetwork of interneurons. We find that this

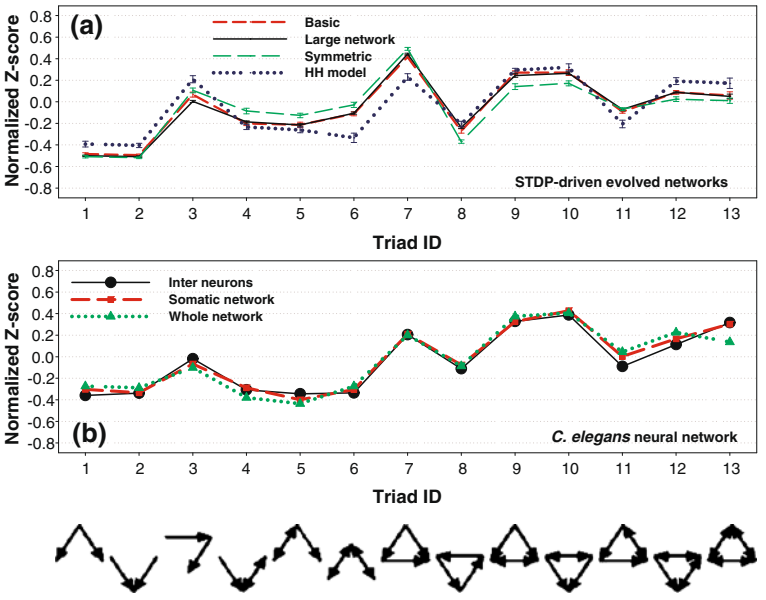

Figure 4. Comparison of SPs for (**a**) four different STDP-driven evolved networks and (**b**) *C. elegans* neuronal networks (the subnetwork of somatic interneurons, the somatic network, the whole neuronal network using the old wiring diagram [15]). We also show the triad subgraph dictionary in this figure.

phenomenon does not depend on the neuron model, the symmetry of the time window or the network size, and thus must reflect some intrinsic characteristic of STDP. Recently, it was shown that the three motifs, feedforward loop (FFL; triad 7) and the mixed-feedforward-feedback loops (MFFL1, MFFL2; triads 9,10) perform important neural computation and cognition tasks in the cell providing an explanation for the abundance of these motifs in the real network [27]. Thus, STDP can develop these important motifs abundant in neuronal networks and characteristic of the second superfamily of [9].

There are small differences between our evolved networks and the subnetwork of interneurons in *C. elegans*: triads 1, 2 and 8 have relatively lower negative SP, while triads 3 and 7 have relatively higher positive SP compared to the *C. elegans* neuronal network (see figure 4). STDP tends to form feedforward structures [28] and reflect the causal relations between neurons, which could lead to over-representation of cascades (triad 3) and FFL (triad 7), and under-representation of cycles (triad 8). On the other hand, we have neglected other mechanisms such as short-term plasticity and hundreds of gap connections that are present in *C. elegans*. The neuron models and parameter setting may also be different from *C. elegans*. Since all these factors could influence the results and have not been accounted in the simulated models, the reported similarities between the evolved and real networks are even more striking. In figure 5 we see that the STDP-driven evolved network for the 'basic configuration' even develops a similar triad frequency spectrum as that of *C. elegans*.

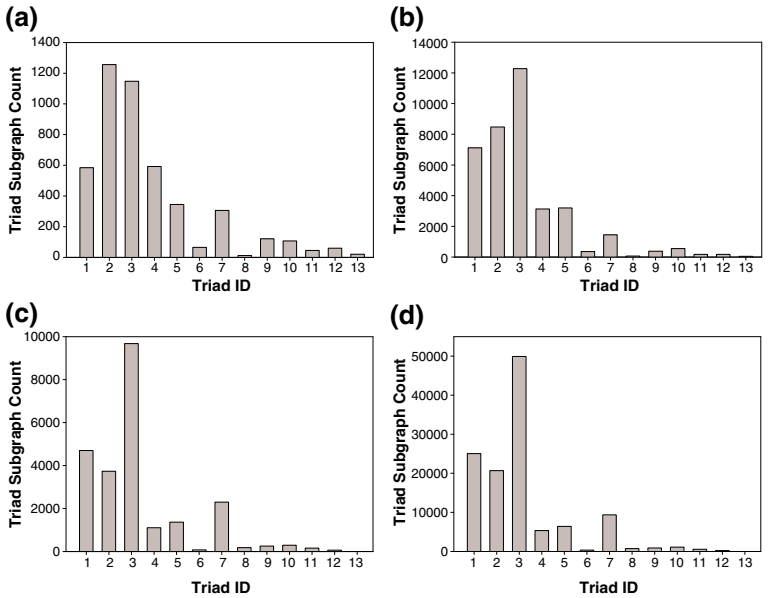

Figure 5. Comparison of triad frequency spectra for STDP-driven evolved networks and *C. elegans* neuronal network. (**a**) Subnetwork of somatic interneurons and (**b**) somatic network in *C. elegans*. STDP-driven evolved networks in (**c**) basic and (**d**) large network configurations.

5. Conclusions

We have studied the effect of a STDP-type learning rule on the structure of the neuronal network. The investigated learning rule incorporates necessary competition between different edges. As the network evolves, some edges grow in strength while other edges become weak. We have considered two types of dynamics on the nodes: (a) A simple nonlinear map, i.e., the logistic map and (b) realistic neuronal dynamics, i.e., leaky integrate and fire (LIF) neuron and Hodgkin–Huxley (HH) models. In logistic map-based model, the edges whose strength become zero are eliminated permanently. This is motivated by the process of pruning in the real biological networks. In realistic LIF and HH models, the strength of edges are allowed to become positive after becoming zero. This accounts for phenomena like exuberance. For all the models, we obtain a residual network with robust properties. The residual network in the case of logistic map is sparser than the one obtained in realistic models. However, it has a broad degree distribution, a property shared by the brain networks.

In the residual network for LIF and HH models, three triads, FFL, MFFL1 and MFFL2, were over-represented compared to randomized networks. These three triads perform important neural computation and cognition tasks. Recently, Meisel and Gross [29] have studied the network with LIF neurons and observed that the networks robustly evolved to a state characterized by the presence of power laws in the distribution of synaptic conductances. Our focus was on the local structure of the resultant network. The SPs of STDP-driven evolved networks are similar to that in the *C. elegans* neuronal network, especially, the subnetwork of interneurons. Also, the triad frequency spectrum of STDP-driven evolved network in certain configurations is similar to that of *C. elegans*. The exact role of neuronal input in determining the network structure is not yet clear but it seems some amount of complexity is needed. This suggests that the learning dynamics plays a crucial role in determining the network structure.

Acknowledgements

KMK acknowledges the support from Department of Science and Technology (DST), India and JJ acknowledges the support from Volkswagen Foundation.

References

[1] R Albert and A-L Barabasi, *Rev. Mod. Phys.* **74**, 47 (2002)
[2] D Watts and S H Strogatz, *Nature* **393**, 440 (1998)
[3] S Bornholdt and H G Schuster, *Handbook of graphs and networks: From the genome to the internet* (Wiley-VCH, Weinheim, 2002)
[4] M E J Newman, *SIAM Rev.* **45**, 167 (2003)
[5] S N Dorogovtsev and J F F Mendes, *Evolution of networks: From biological nets to the internet and WWW* (Oxford University Press, USA, 2003)
[6] V M Eguíluz, D R Chialvo, G A Cecchi, M Baliki and A V Apkarian, *Phys. Rev. Lett.* **94(1)**, 018102 (2005)
[7] C J Stam and J C Reijneveld, *Nonlin. Biomed. Phys.* **1**, 3 (2007)
[8] R Milo, S Shen-Orr, S ltzkovitz, N Kashtan, D Chklovskii and U Alon, *Science* **298**, 824 (2002)

[9] R Milo, S Itzkovitz, N Kashtan, R Levitt, S Shen-Orr, I Ayzenshtat, M Sheffer and U Alon, *Science* **303**, 1538 (2004)
[10] J Jost and K M Kolwankar, *Physica* **A388**, 1959 (2009)
[11] Q Ren, K M Kolwankar, A Samal and J Jost, *Physica* **A389**, 3900 (2010)
[12] G Shepherd, *Neurobiology* (Oxford Univ. Press, 1994)
[13] D L Bishop, T Misgeld, M K Walsh, W Gan and J W Lichtman, *Neuron* **44(4)**, 651 (2004)
[14] W Wadsworth, *Curr. Biol.* **15**, R796 (2005)
[15] J G White, E Southgate, J N Thomson and S Brenner, *Phil. Trans. R. Soc. London* **B314**, 1 (1986)
[16] L R Varshney, B L Chen, E Paniagua, D H Hall and D B Chklovskii, *PLoS Comput. Biol.* **7**, e1001066 (2011)
[17] R K Pan, N Chatterjee and S Sinha, *PLoS ONE* **5(2)**, e9240 (2010)
[18] N Chatterjee and S Sinha, *Progress in brain research* (Elsevier, 2008) Vol. 168, pp. 145–153
[19] E L Peckol, J A Zallen, J C Yarrow and C I Bargmann, *Development* **126**, 1891 (1999)
[20] H Markram, J Lübke, M Frotscher and B Sakmann, *Science* **275**, 213 (1997)
[21] T Wennekers and N Ay, *Neural Comput.* **17**, 2258 (2005)
[22] M-O Gewaltig and M Diesmann, *Scholarpedia* **2(4)**, 1430 (2007)
[23] S Song, K D Miller and L F Abbott, *Nature Neurosci.* **3(9)**, 919 (2000)
[24] R D Traub and R Miles, *Neuronal networks of the hippocampus* (Cambridge University Press, Cambridge, UK, 1991)
[25] C-W Shin and S Kim, *Phys. Rev*. **E74**, 045101(R) (2006)
[26] G Bi and M Poo, *Annu. Rev. Neurosci.* **24**, 139 (2001)
[27] C Li, *Phys. Rev*. **E78**, 037101 (2008)
[28] N Masuda and H Kori, *J. Comput. Neurosci.* **22**, 327 (2007)
[29] C Meisel and T Gross, *Phys. Rev.* **E80**, 061917 (2009)